



Article

Column Adsorption Studies for the Removal of Ammonium Using Na-Zeolite-Based Geopolymers

Elavarasi Sundhararasu ¹, Hanna Runtti ¹, Teija Kangas ¹, Janne Pesonen ¹, Ulla Lassi ^{1,2} and Sari Tuomikoski ^{1,*}

¹ Research Unit of Sustainable Chemistry, University of Oulu, P.O. Box 4300, FI-90014 Oulu, Finland

² Unit of Applied Chemistry, Kokkola University Consortium Chydenius, University of Jyväskylä, Talonpojankatu 2B, FI-67100 Kokkola, Finland

* Correspondence: sari.tuomikoski@oulu.fi

Abstract: The aim of this study was to examine the removal of ammonium ions from a synthetic model solution by using Na-zeolite-based geopolymers. Na-zeolite (=analcime) is a residue from mining industry. Three adsorbents were prepared from Na-zeolite using different production steps and metakaolin as a blending agent. These novel adsorbents were investigated in a fixed-bed column system where the effects of different flow rates with the initial ammonium concentration of 40 mg/L were studied. The Thomas, Bohart–Adams and Yoon–Nelson breakthrough curve models fitted well with the experimental data with a high R^2 value. After adsorption experiments, adsorbents were regenerated using a mixture of 0.2 M NaCl and 0.1 M NaOH as a regeneration agent; after that, adsorbents were reutilised for ammonium ion adsorption for three adsorption–regeneration cycles. The results of the experiment indicate that all the prepared analcime-based geopolymers are suitable adsorbents for the removal of ammonium ions and that capacity remains nearly constant for two of them during two adsorption–regeneration cycles.

Keywords: geopolymer; fixed-bed column; ammonium ion; breakthrough models; regeneration



Citation: Sundhararasu, E.; Runtti, H.; Kangas, T.; Pesonen, J.; Lassi, U.; Tuomikoski, S. Column Adsorption Studies for the Removal of Ammonium Using Na-Zeolite-Based Geopolymers. *Resources* **2022**, *11*, 119. <https://doi.org/10.3390/resources11120119>

Academic Editors: Eva Pongrácz, Cara Beal, Kazuyo Matsubae, Jenni Ylä-Mella and Sherien Elagroudy

Received: 31 October 2022

Accepted: 8 December 2022

Published: 11 December 2022

Publisher's Note: MDPI stays neutral with regard to jurisdictional claims in published maps and institutional affiliations.



Copyright: © 2022 by the authors. Licensee MDPI, Basel, Switzerland. This article is an open access article distributed under the terms and conditions of the Creative Commons Attribution (CC BY) license (<https://creativecommons.org/licenses/by/4.0/>).

1. Introduction

During wastewater treatment, contaminants are removed from water using biological, physical and mechanical processes [1,2]. Even though ammonium is an essential nitrogen-containing nutrient, a high amount of ammonium affects water quality and ecosystems [3]. Agricultural, industrial or municipal wastewater sources are major sources of ammonium-caused pollution problems. Industrial processes need to be improved by treating wastewater to prevent pollution [1,4]. High levels of ammonium in wastewater affect natural nitrification activity. There are also European Council directives regarding urban wastewater treatment, which state that 70–80% of nitrogen from wastewater should be removed [5].

Currently, various methods are used for the removal of ammonium from wastewater, such as ion exchange [1], biological nitrification–denitrification [6], chemical precipitation [7] and air stripping [8]. They all have their advantages and disadvantages. Air stripping is widely used under alkaline conditions in wastewater treatment but it is not an energy-efficient method, and it is also not sensitive to substances that are toxic [2]. The chemical precipitation method is a simple and cost-effective process for wastewater treatment but uses extra reagents for the treatment process and generates new pollutants in water due to the usage of salt for precipitation [2,9–11]. Widely used biological methods are effective but they are not suitable for high ammonium load because removal of accumulated nitrate cause additional costs [2,12]. Biochar-based materials should be integrated with biological treatments to improve the effective removal of various contaminants (such as nitrate, phosphate, ammonia nitrogen and chloride) [13]. Chemical precipitation

and microbiological methods are characterized by processing complexities and high operational costs, and it has also been demonstrated that in practical applications microorganisms have a lower rate of survival [2,14,15]. Air stripping and similar denitrification processes are not simple to set up and are affected by low temperatures [7]. Due to the simplicity of the processes and the fact that they are not affected by low temperatures, ion exchange and adsorption methods are effective in the removal of ammonium ions [2,7]. These are a few examples of the advantages and disadvantages of the currently available methods for the separation of ammonium from wastewater.

The adsorption method is a simple process for reducing and removing contaminants where the adsorbent is usually used to adsorb pollutants from wastewater [16]. Adsorption could be based on ion exchange, physisorption or chemisorption [17,18]. Gao et al. (2020) have reported that ammonium removal was based on chemisorption [19]. Compared to traditional ammonium-removal methods, the adsorption and ion exchange methods have more advantages because they are environmentally friendly processes, use simple adsorbent production technology and are also cost-effective when adsorbents can be prepared from industrial by-products [2,20]. Activated carbon has been commonly used as an effective adsorbent [2]. In activated carbon, the adsorption capacity can be improved, e.g., by using different surface modification methods like surfactants [21]. However, geopolymers are considered to be more cost-effective adsorbents and contribute to sustainable wastewater treatment processes [17,18].

Geopolymers are described as amorphous, non-crystalline structures produced through the reaction between aluminosilicate-containing precursors and alkaline activators at an ambient temperature. The chemical structure of geopolymers makes them suitable as efficient adsorbents in wastewater treatment since their structure consists of an alumina silicate framework which is negatively charged and is characteristic of interchangeable charge-balancing behaviour in the activator solution [22–25]. The process of charge balancing in the Na^+ cations of the geopolymer aluminosilicate results in the exchange of ammonium ions up to around 100%, which shows the high affinity nature of geopolymers for ammonium ion [4,18,23,26]. The geopolymer preparation process is simpler than that of traditional adsorbents (e.g., zeolite, activated carbon and resin) due to the low temperature used and, for example, the use of non-hazardous chemicals. In addition, the adsorption process is simple and effective [17,23,27–29].

Zeolites can be used in wastewater treatment to remove heavy metals using the ion exchange method. These adsorbents are cost-effective and found naturally in salt lakes, volcanic environments and sediment layers. Na-zeolite is abbreviated to analcime in this paper. Analcime (ANA), clinoptilolite, phillipsite and dachiardite are some of the most common types of zeolites. Zeolites belong to the crystalline hydrated aluminosilicates family and have properties such as the exchangeability of anions and cations. Currently, clinoptilolite is widely used for wastewater treatment due to its good availability [30–32]. Recent experiments show that analcime has adsorbent properties and can be used to remove ammonium ions from wastewater. ANA $[\text{Na}_{16}(\text{Al}_{16}\text{Si}_{32}\text{O}_{96}) \cdot 16\text{H}_2\text{O}]$ is formed as a side stream during the production of lithium carbonate from spodumene ($\text{LiAlSi}_2\text{O}_6$) using a sodium pressure-leaching process [33]. In recent years, metakaolin, a type of calcinated clay, has also been used as an adsorbent. Although it is not efficient as an adsorbent in the removal of ammonium ions without any treatment, geopolymerisation improves the ammonium removal capacity [4]. In this work, analcime from industrial mining and metakaolin have been studied and used as the raw materials for geopolymerization.

Apart from the widely used batch-adsorption method, the fixed-bed column method is also broadly used in the contaminant removal process. In this method, the adsorbate is left to flow continuously over plastic or glass columns. This method is preferred because of its efficiency in managing differences in large concentrations; it can also be scaled up to meet industrial standards [16,34,35]. Several empirical methods, such as the Thomas, Yoon–Nelson and Bohart–Adams models, are generally applied to column adsorption data to determine breakthrough behaviour [16,36,37].

In this study, three geopolymer materials were prepared using analcime and metakaolin as raw materials. To measure the capacity of the prepared materials for ammonium ion removal, experiments were performed for ammonium ion removal and the effect of flow rate was studied. After the adsorption experiments, the stability of the adsorbent materials was studied by performing regeneration experiments. The experimental data obtained from the fixed-bed columns were applied using mathematical models: Thomas, Yoon–Nelson and Bohart–Adams. This study utilises inexpensive industrial side streams and investigates the possibility of the creation of a low-cost and simple approach to the removal of ammonium from synthesised wastewater.

2. Materials and Methods

2.1. Chemicals

Analcime was obtained from lithium carbonate production through a Finnish mining company. Metakaolin samples were obtained from Aquaminerals Finland Ltd (Paltamo, Finland). The synthetic wastewater solution was prepared using ammonium hydroxide (obtained through VWR International, Radnor, PA, USA). Hydrochloric acid and sodium hydroxide were used for pH value moderation and hydrochloric acid for the acid washing of the analcime (these were obtained through FF Chemicals, Werkendam, The Netherlands). An alkaline solution of sodium silicate, sodium hydroxide and potassium silicate (obtained through VWR international, Radnor, PA, USA) was utilised in the synthesis of the geopolymers. In this study, three different kinds of alkaline solution combinations have been used for the preparation of geopolymers. Sodium chloride and sodium hydroxide were purchased from VWR International Chemicals and used as regeneration agents.

2.2. Characterisation Techniques and Analytical Methods

The pore size, volume and the specific surface area were calculated from nitrogen gas adsorption–desorption isotherms. The experiment was carried out using Micromeritics ASAP 2020 equipment with liquid nitrogen ($-196\text{ }^{\circ}\text{C}$). The Brunauer–Emmett–Teller (BET) formula was used to calculate specific surface area and the Barrett–Joyner–Halenda (BJH) method was used to calculate the pore surface size distribution from the desorption data. The $\text{NH}_4\text{-N}$ concentration was analysed using the Hach HQ30d equipped with an ammonium ion-selective electrode. pH measurements were also conducted using the Hach HQ30d.

2.3. Preparation of Analcime-Based Geopolymers

Sodium hydroxide, sodium silicate and potassium silicate alkaline solutions were used for synthesising geopolymers in this study. Before alkaline activation, the raw material particle size was $<1\text{ mm}$. GEOP1 was synthesised by adding sodium hydroxide and sodium silicate (1:1) to the analcime and metakaolin (ratio 3:1). GEOP2 was prepared from analcime by adding sodium silicate and water for the mixing of the sample. Before alkaline activation, the analcime sample was first washed in 2 M of hydrochloric acid for 24 h. After washing, the samples were kept in the oven at $105\text{ }^{\circ}\text{C}$ for 24 to 48 h for drying. In the formation process of GEOP3, In the formation process of GEOP3, a weight ratio of 3:1 analcime and metakaolin were mixed with sodium hydroxide and potassium hydroxide (1:1). After alkaline activation the sample was poured into the silica mould and kept at room temperature for three days. De-moulded samples were crushed using a jaw crusher and sieved into $<150\text{ }\mu\text{m}$ particles. All the prepared geopolymers were washed with distilled water to eliminate unreacted alkaline solution and were dried overnight in an oven at $105\text{ }^{\circ}\text{C}$.

2.4. Column Experiments

The fixed-bed column system was constructed using a plastic column (diameter 3 cm, height 7 cm), where the ammonium solution continuously flowed from bottom to top with the aid of a roller pump (Watson–Marlow 120 Series). At the bottom of the column, the

deposited plastic sieve was followed by glass wool. Three grams (0.5 cm) of geopolymer adsorbent was placed in the fixed-bed column. To prevent the loss of adsorbent during the experiment, adsorbent was surrounded with acid-washed fine and normal sand [28]. Adsorption behaviour was studied with flow rates of 5, 10 and 20 mL/min at room temperature. The target concentration of the ammonium solution was 40 mg/L and the bed height was 0.5 cm in all experiments. The column set-up has been presented in more detail in our previous work [28]. The kinetics of the adsorption process were followed by collecting samples from the effluent at specific time intervals. The initial pH was adjusted to 2.5 but it increased up to 7–8 during the experiment. Alkaline pH was avoided since the NH_4^+ ions tend to evaporate as ammonia in high pH values (NH_4^+ pK_a value is 9.24) [18,38]. The adsorption method depends on the pH value of the effluent, as the H^+ ions compete with NH_4^+ ions when the pH value is low. Ammonium ion concentrations were examined using an ammonium-selective electrode. When the ammonium ion concentration was above 99% of the incoming ammonium concentration, the continuous flow of the synthetic model solution was stopped and distilled water was poured through the column.

Breakthrough curves were determined as an action of different ammonium concentration and the flow rate depended on the ratio of outlet and inlet concentration (C/C_0) at a function of outflow time (t). The maximal adsorption capacity q_{total} (mg) in the column was estimated by integrating the plot of metal adsorbed concentration versus the outflow time (t). The adsorbed concentration for metal can be determined from the breakthrough curve ($C_{ad} = C_0 - C$) using the equation:

$$q_{total} = \frac{QA}{1000} = \frac{Q}{1000} \int_{t=0}^{t=t_{total}} C_{ad} dt \quad (1)$$

where C_0 and C denote the initial inlet and outlet concentration (mg/L), respectively. A is the area above the breakthrough curve, Q refers to the flow rate (mL/min) and t_{total} represents the total time for the fixed-bed column to reach saturation of adsorbent with ammonium ions (min).

The equilibrium capacity (q_e) was determined using the fixed-bed column data (mg/g), through the ratio of the total amount of ammonium ions adsorbed into the adsorbent q_{total} (mg) and the dry weight of analcime geopolymer used in the adsorbent bed (g):

$$q_e = \frac{q_{total}}{m} \quad (2)$$

2.5. Regeneration

Analcime geopolymers were regenerated after each adsorption. In total, three adsorption–regeneration cycles were implemented during this study. After the adsorption experiment, the adsorbate solution was completely removed from the column by washing it with 1 L of distilled water for 1 h using a 20 mL/min flow rate. After washing, the mixture of 0.1 M of sodium hydroxide and 0.2 M of sodium chloride with a weight ratio of 1:3 was used to regenerate the adsorption material. The regeneration experiment was performed at room temperature. The experiment was stopped when the effluent reached inlet concentration.

2.6. Breakthrough Curve Modelling

Generally used models—the Bohart–Adams, Thomas and Yoon–Nelson models—were employed to describe the adsorption process. Details concerning these models are presented in the following sections. Models have been applied to an increasing part of the breakthrough curves and parameters have been implemented to draw conclusions from the experimental data and define the behaviour of the fixed-bed column. All the models used are based on the same general equation [37] and therefore they all have equal R^2 value.

2.6.1. Thomas Model

The Thomas model is widely used for column experimental data to investigate the prospect of breakthrough curves. This model evolved assuming the Langmuir kinetics of adsorption–desorption and second-order reversible reaction kinetics [39]. Any axial dispersion does not derive from adsorption. The Thomas model is more applicable for a sorption process when internal and external diffusion limitations are absent. The adsorption capacity and rate constant were appraised by the Thomas model in fixed-bed column methods [36,37,40].

The linearised form of the Thomas model can be given as:

$$\ln\left(\frac{C_0}{C} - 1\right) = \frac{k_T q_0 m}{Q} - k_T C_0 t \quad (3)$$

where k_T indicates the Thomas rate constant (mL/min·mg), q_0 is the equilibrium uptake capacity of the adsorbent (mg/g), m is mass of adsorbent (g), Q (mL/min) is the flow rate of the bed, C is the outlet ammonium concentration (mg/g), C_0 is the inlet ammonium concentration (mg/g) and term t is the sampling time (min). The values of k_T and q_0 are calculated from the plot of $\ln[(C_0/C_t)^{-1}]$ against t .

2.6.2. Bohart–Adams Model

The Bohart–Adams model [41] is used to describe the ratio between concentration (C_0/C) as mg/g and time t (min) in the fixed-bed column system. The model has been used to describe the initial part of the breakthrough curve. It describes the adsorption rate dependent on the metal concentration of the adsorbing species and the residual capacity of the adsorbent in the column. The Bohart–Adams model was applied to determine the adsorption capacity and the service time based on the column bed height at different flow rates [36,37,40]. The Bohart–Adams model can be expressed as follows:

$$\ln\left(\frac{C_0}{C} - 1\right) = \frac{k_{BA} N_0 h}{v_F} - k_{BA} C_0 t \quad (4)$$

where k_{BA} is the rate constant (L/mg min), N_0 denotes the saturation concentration (mg/L), h represents the bed height (cm), v_F refers to linear flow velocity (cm/min) and t denotes time (min).

2.6.3. Yoon–Nelson Model

The Yoon–Nelson model considers that the decrease rate of each molecule's adsorption probability will be directly proportional to the adsorbate's adsorption probability and the breakthrough probability of the adsorbate on the adsorbent [42]. Adsorption probability will be proportional directly to the adsorbate adsorption probability and the breakthrough probability of adsorbate on the adsorbent [42]. This model does not emphasise the type of the adsorbent or the adsorbate characteristics or the fixed-bed column's parameters. [36,37,40]. The equation of this model is expressed as:

$$\ln\left(\frac{C_0}{C} - 1\right) = k_{YN}(\tau - t) \quad (5)$$

where k_{YN} represents the Yoon–Nelson rate constant (L/min), τ refers to the time required for 50% of ammonium ion breakthrough (min) and t shows the breakthrough time (min).

3. Results and Discussion

3.1. Characterisation of the Adsorbent

The specific surface area, pore size and pore volume are listed in Table 1. The highest pore size was found for GEOP 1 and lowest surface areas for GEOP1. Each sorbent displayed the characteristic of having a mesopore structure. Pore size of the analcime-

based geopolymer are higher than NaP zeolite adsorbents (3.0 nm) [43] and coal-analcime adsorbents (9.02 nm) [44]. Non modified analcime has lower surface area (3.01 m²/g) than analcime-based geopolymers [45]. Geopolymers usually act as effective ion exchangers [17] and surface area does not have much of an effect in adsorption. However, this study's results show that the surface area of the material enables ion exchange as the surface of the sample has mesoporosity, which contributes to the adsorption capacity of ammonium ion.

Table 1. Specific surface areas, pore sizes and pore volumes for prepared analcime-based geopolymers.

Adsorbent	Specific Surface Area [m ² /g]	Average Pore Diameter [nm]	Cumulative Pore Volume [cm ³ /g]
GEOP 1	4.180	31.281	0.257
GEOP 2	10.981	22.494	0.329
GEOP3	7.784	12.831	0.302

3.2. Effect of Operating Conditions

The effect of flow rate on ammonium removal was investigated at three flow rates (5, 10 and 20 mL/min) by using a fixed-bed height of 0.5 cm and an initial inlet ammonium concentration of 40 mg/L. The breakthrough curves are illustrated in Figure 1. With higher flow rates, the amount of ammonium passing the adsorbent is high and saturation is reached sooner. This leads to a sharper curve [46]. When residence time is increased, ammonium has more time to diffuse on the pores of the analcime geopolymer, allowing ammonium ions to approach more binding sites in the adsorbent. Three adsorbent materials did not show a significant difference in terms of adsorption performance. Surface of the adsorbent was occupied slightly faster in the case of GEOP1 and GEOP2 than in the case of GEOP3. This could be explained by the pore sizes of the prepared adsorbent materials. The size of ammonium ion is (1.54 Å = 15.4 nm), larger than the pore diameter of GEOP3, whereas ammonium can occupy pores of GEOP1 and GEOP2 because of its clearly smaller diameter than the pore sizes of the adsorbents. Kizito et al. (2016) investigated the effect of flow rate (15 mL/min to 25 mL/min) with inlet NH₄-N concentration from 500 mg/L to 585 mg/L and bed height 60 cm and used three types of biochar which have been made from corncobs (MCB), hardwood (WB) and pellets of mixed sawdust in fixed-bed column experiments. This experiment confirmed that lower flow rates increased the saturation time and thus active sites of the inter particle diffusion are better and resulted in lasting bed saturation time. These results show that the maximum adsorption capacity depends on ammonium concentration (500 mg/L) and lower flow rates (15 mL/min) [34]. Nguyen et al. (2019) studied varying initial ammonium concentrations (10 to 40 mg/L), flow rates (1 to 9 mL/min) and bed heights (8–24 cm), which used corncob based on modified biochar in column studies. With high ammonium concentration, lower bed height and higher flow rate, the column experiment process was controlled by internal mass transfer; this speeds up the ammonium diffusion in the column, which helps to reach the exhaust time and breakthrough earlier [47].

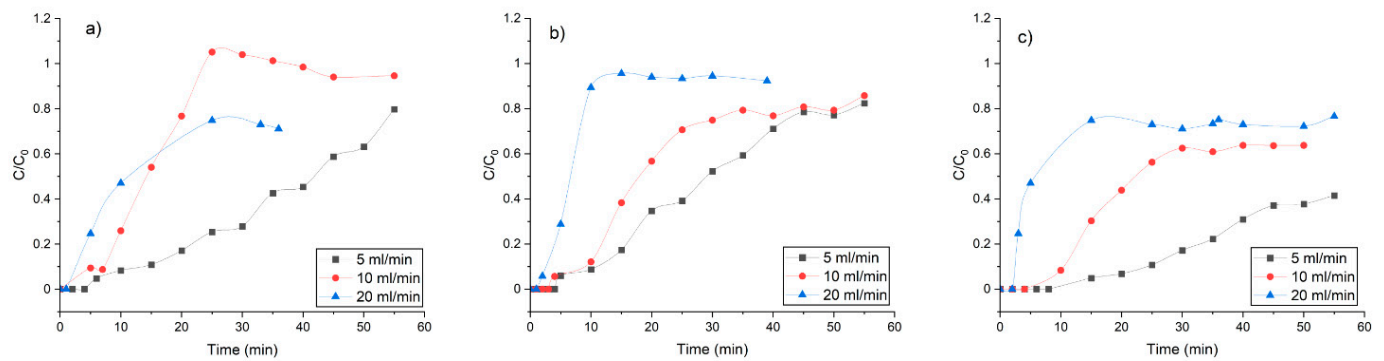


Figure 1. Effect of flow rates on breakthrough curves for ammonium adsorption on analcime geopolymer at a fixed-bed height of 0.5 cm and a concentration of 40 mg/L. (a) GEOP1; (b) GEOP2; (c) GEOP3.

3.3. Breakthrough Curve Models

The parameters of the Thomas, Bohart–Adams and Yoon–Nelson models are presented in Table 2. Experimental q values have also been included for comparison. High R^2 values indicate a good fit of the models and the values ranged from 0.897 to 0.999. GEOP1 has slightly larger q values than GEOP2 and GEOP3. The experimental and theoretical q values are in same order of magnitude and decrease when the flow rate increases, showing that the adsorption phases (external surface adsorption, pore diffusion) need time to take place. However, reaction rates (k_T , k_{BA} , k_{YN}) increase with the flow rates, indicating that the capacity of the adsorbent is possibly used more effectively with the larger flow rates. Fifty per cent saturation of the adsorbent surface (τ) is reached more slowly when the flow rates are smaller. Similar results have been reported previously regarding ammonium removal with different kinds of adsorbents (e.g., biochar) [34,47,48]. Higher flow rates shorten the saturation time.

Table 2. Parameters of the Thomas, Bohart–Adams and Yoon–Nelson models and experimental adsorption capacities at different flow rates at a fixed-bed height of 0.5 cm and a concentration of 40 mg/L.

Adsorbents	Thomas Model		Bohart–Adams Model		Yoon–Nelson Model		R^2		
	Q [mL/min]	q_e (mg/g)	$k_T \times 10^{-3}$ [L/min mg]	q_0 [mg/g]	$k_{BA} \times 10^{-3}$ [L/mg min]	v_F [cm/min]		k_{YN} [L/min]	τ [min]
GEOP1	5	3.264	1.550	3.361	1.550	0.0101	0.0799	40.860	0.991
	10	2.198	5.884	2.303	5.884	0.0324	0.2645	14.934	0.976
	20	2.200	12.887	1.788	12.887	0.0617	0.4433	7.308	0.967
GEOP2	5	2.102	3.220	1.813	3.220	0.0152	0.1017	30.509	0.978
	10	2.071	7.231	1.612	7.231	0.0203	0.1865	19.250	0.951
	20	2.019	14.189	2.034	14.189	0.0708	0.6144	6.515	0.999
GEOP3	5	2.101	1.946	2.153	1.946	0.0038	0.0546	67.132	0.897
	10	2.067	6.171	2.009	6.171	0.0152	0.2133	20.410	0.936
	20	1.346	12.841	1.147	12.841	0.0624	0.3467	5.854	0.984

3.4. Adsorption and Regeneration Studies

During the adsorption experiment, the analcime-based geopolymer was saturated. After the experiment, the adsorbent material in the column regenerated using NaOH and NaCl as regeneration agents. The effectiveness of regeneration was tested by implementing three adsorption–desorption cycles, i.e., repeating the adsorption experiment and comparing the adsorption capacities of consecutive adsorption experiments. The adsorption–regeneration cycle was repeated so that two cycles were performed after the

first adsorption experiment. The result of the adsorption experiments after regeneration have been compared to the results of the first adsorption experiment in Figure 2.

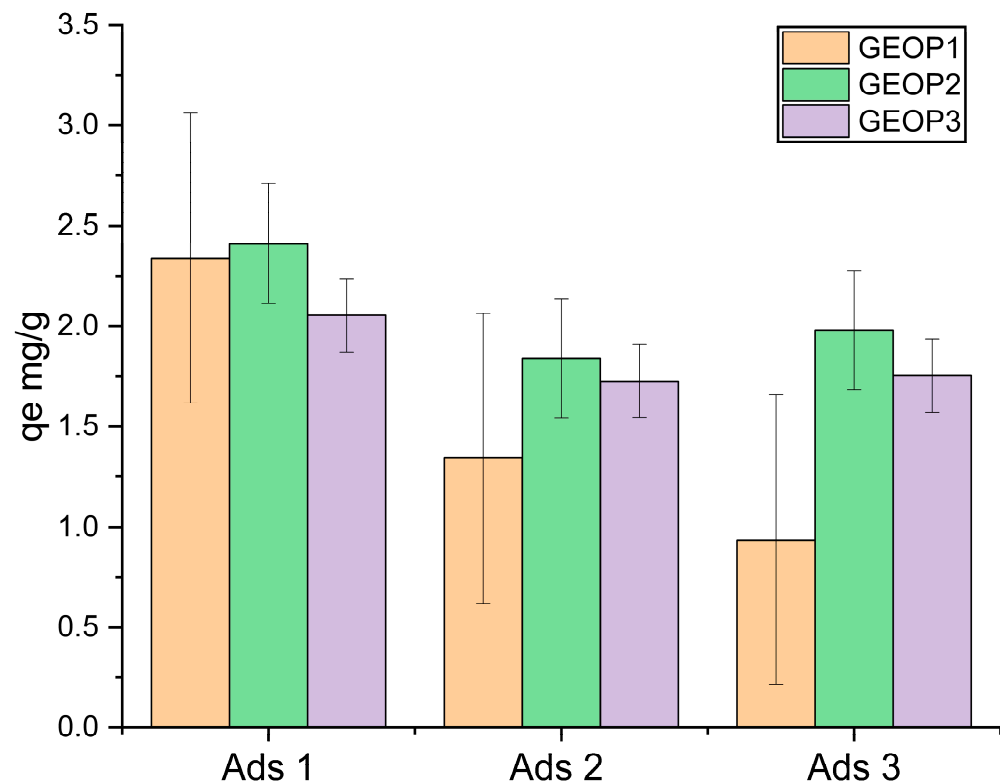


Figure 2. Saturation capacity for adsorption–desorption cycles.

Fixed-bed column regeneration studies were performed using a flow rate of 20 mL/min, a concentration of 40 mg/L and a fixed-bed height of 0.5 cm. In the case of GEOP2 and GEOP3, adsorption capacities during the regeneration cycles remained almost constant, with only a small decrease after the first cycle. However, the adsorption capacity of GEOP1 clearly decreased during the cycles, indicating that the material cannot be regenerated effectively. The capacity of GEOP2 and GEOP3 even increases slightly in the third cycle. Breakthrough curves from the different adsorption cycles are presented in Figure 3. The results confirm that sodium-based desorption solvent worked as a regeneration agent for ammonium ions from the saturated analcime geopolymer GEOP1, GEOP2 and GEOP3.

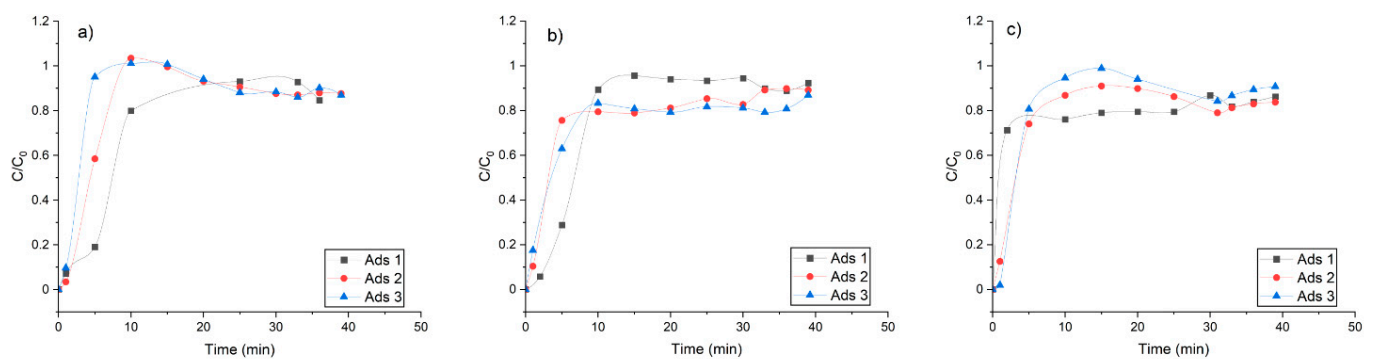


Figure 3. Breakthrough curves for adsorption–regeneration into the analcime geopolymer at 20 mL/min flow rate and a fixed-bed height of 0.5 cm. (a) GEOP1; (b) GEOP2; (c) GEOP3.

3.5. Evaluation of Achieved Results

In this study, three adsorbents were prepared using varying methods from the metal mining industry side stream, analcime. Pore size of the GEOP1 and GEOP2 enables the diffusion of ammonium ions to the pores of adsorbents, supporting the adsorption mechanism [2]. However, GEOP3 obtained almost as high a q value as GEOP2 and only slightly smaller than GEOP1, which could indicate other mechanisms (e.g., ion exchange) [18,49].

Currently, most research results reported in the literature focus on batch experiments, while only a few studies concentrate on fixed-bed column experiments. The adsorption capacities achieved for ammonium ions in fixed-bed column studies using aluminosilicate-based adsorbent materials are compared in Table 3. Due to the varying nature of experimental conditions, it is difficult to compare the q values achieved in different studies. Results shows that Chinese zeolite has a comparably high adsorption capacity and modified sand has minor adsorption capacity, but all other values are approximately in the same order of magnitude. The values achieved in this study are in the smaller part of the range. However, the adsorption materials in this study were drawn from industrial side streams and would be wasted if they were not used in water treatment. Using raw materials retrieved from side-stream material brings added value to the study from the standpoint of the circular economy when compared with using commercial raw materials or virgin materials.

In the literature, the effect of coexisting ions for ammonium adsorption was also studied. Xiong et al. (2023) found that ammonium and phosphorus can be removed at the same step by using low-grade sepiolite as an adsorbent. They found that initial nutrient concentrations 30 mg/L N/L and 100 mg P/L can be removed to the level of 5 mg N/L and 0.5 mg P/L. [50] Samarina et al. (2022) found that geopolymer-based adsorbents from fly ash and metakaolin can remove ammonium from run-off mine wastewater that also include other elements besides ammonium [51]. Karadag et al. (2008) removed ammonium from municipal landfill leachate by clinoptilolite and found a decrease of ammonium ion from 3000 mg/L to 400 mg/L [52]. Therefore, ammonium can typically be removed from solutions including several ions. However, the effect of coexisting ions was not considered in this study.

Table 3. Comparison of the maximum adsorption capacity of analcime-based geopolymer adsorbent with different adsorbent for fixed-bed column studies.

Adsorbent	Mass of Adsorbent [g]	Bed Height [cm]	Flow Rate [mL/min]	Initial Concentration [mg/L]	pH	Adsorption Capacity [mg/g]	References
Jordanian natural zeolite	53–206	10–40	100–250	15–50	5.5–9	3.9–5.32	[53]
Chinese zeolite	-	28		250		9.1–9.6	[30]
Clinoptilolite	600	40	6.8–21	100–400	12	4.69–5.77	[52]
Functionalized Zeolites	10	-	2	50		7.95	[31]
Modified sand	996	80	20	-	7	0.014	[54]
GEOP1	3	0.5	5–20	40	2.5	3.264–2.20	This study
GEOP2	3	0.5	5–20	40	2.5	2.102–2.019	This study
GEOP3	3	0.5	5–20	40	2.5	2.101–1.346	This study

4. Conclusions

The removal of ammonium ions in the synthetic model solution was performed by using analcime geopolymer in a fixed-bed column study. The effect of flow rate (5, 10, 20 mL/min) with fixed-bed height (0.5 cm) and concentration (40 mg/L) were examined in the column study, which revealed a significant change in the rate of adsorption. Column adsorption capacity increased with a decreased flow rate and saturation capacities of 1.788 to 3.361 for GEOP1, 1.612 to 2.034 for GEOP2 and 1.147 to 2.153 for GEOP3, respectively. A higher flow rate resulted in steeper breakthrough curves. The experimental data obtained from the study fitted well with the Bohart–Adams, Thomas and Yoon–Nelson models. A mixture of 0.1 M NaOH and 0.2 M NaCl was used to regenerate the ammonium-

loaded adsorbents. Three cycles of this process were repeated, and it was observed that there was only a small decrease in adsorption capacities after regeneration. Future studies should focus on industrial scale usage and investigate a few aspects such as adsorbent dosage and initial metal concentration.

Author Contributions: Conceptualization, E.S.; methodology, E.S.; software, T.K., H.R. and E.S.; investigation, E.S., and J.P.; data curation, E.S., H.R., T.K. and S.T.; writing—original draft preparation, E.S.; writing—review and editing, E.S., S.T., H.R., T.K., J.P. and U.L.; visualization, E.S., H.R., S.T., J.P. and T.K.; supervision, S.T., H.R. and U.L.; project administration, U.L.; funding acquisition, E.S. and U.L. All authors have read and agreed to the published version of the manuscript.

Funding: This work was supported by Maa-ja Vesitekniiikan tuki ry and conducted as part of WaterPro (ERDF Project No. A74635, funded by the Central Ostrobothnia Regional Council, the European Union, the European Regional Development Fund, and the Leverage from the EU).

Data Availability Statement: The data presented in this study are available within the article (tables and figures). The data presented in this study are available on request from the corresponding author.

Acknowledgments: The authors would like to thank Toni Varila for his assistance in the characterization of the samples.

Conflicts of Interest: Authors declare no conflict of interest. The funders had no role in the design of the study; in the collection, analyses, or interpretation of data; in the writing of the manuscript, or in the decision to publish the results.

References

1. Zhao, C.; Zheng, Z.; Zhang, J.; Wen, D.; Tang, X. Adsorption Characteristics of Ammonium Exchange by Zeolite and the Optimal Application in the Tertiary Treatment of Coking Wastewater Using Response Surface Methodology. *Water Sci. Technol.* **2013**, *67*, 619–627. [[CrossRef](#)] [[PubMed](#)]
2. Huang, J.; Kankanamge, N.R.; Chow, C.; Welsh, D.T.; Li, T.; Teasdale, P.R. Removing Ammonium from Water and Wastewater Using Cost-Effective Adsorbents: A Review. *J. Environ. Sci.* **2018**, *63*, 174–197. [[CrossRef](#)] [[PubMed](#)]
3. Rožić, M.; Cerjan-Stefanović, Š.; Kurajica, S.; Vančina, V.; Hodžić, E. Ammoniacal Nitrogen Removal from Water by Treatment with Clays and Zeolites. *Water Res.* **2000**, *34*, 3675–3681. [[CrossRef](#)]
4. Luukkonen, T.; Sarkkinen, M.; Kempainen, K.; Rämö, J.; Lassi, U. Metakaolin Geopolymer Characterization and Application for Ammonium Removal from Model Solutions and Landfill Leachate. *Appl. Clay Sci.* **2016**, *119*, 266–276. [[CrossRef](#)]
5. Prabesh, K.C. *New Opportunities of Nutrient Recycling in Water Services*; Hämeen Ammattikorkeakoulu: Hämeenlinna, Finland, 2018; ISBN 9789517847872.
6. Hwang, J.H.; Oleszkiewicz, J.A. Effect of Cold-Temperature Shock on Nitrification. *Water Environ. Res.* **2007**, *79*, 964–968. [[CrossRef](#)]
7. Huang, H.; Yang, L.; Xue, Q.; Liu, J.; Hou, L.; Ding, L. Removal of Ammonium from Swine Wastewater by Zeolite Combined with Chlorination for Regeneration. *J. Environ. Manag.* **2015**, *160*, 333–341. [[CrossRef](#)]
8. Guštin, S.; Marinšek-Logar, R. Effect of PH, Temperature and Air Flow Rate on the Continuous Ammonia Stripping of the Anaerobic Digestion Effluent. *Process Saf. Environ. Prot.* **2011**, *89*, 61–66. [[CrossRef](#)]
9. Zhang, T.; Li, Q.; Ding, L.; Ren, H.; Xu, K.; Wu, Y.; Sheng, D. Modeling Assessment for Ammonium Nitrogen Recovery from Wastewater by Chemical Precipitation. *J. Environ. Sci.* **2011**, *23*, 881–890. [[CrossRef](#)]
10. Huang, H.; Huang, L.; Zhang, Q.; Jiang, Y.; Ding, L. Chlorination Decomposition of Struvite and Recycling of Its Product for the Removal of Ammonium-Nitrogen from Landfill Leachate. *Chemosphere* **2015**, *136*, 289–296. [[CrossRef](#)]
11. Chen, Y.; Xiong, C.; Nie, J. Removal of Ammonia Nitrogen from Wastewater Using Modified Activated Sludge. *Polish J. Environ. Stud.* **2016**, *25*, 419–425. [[CrossRef](#)]
12. Feng, S.; Xie, S.; Zhang, X.; Yang, Z.; Ding, W.; Liao, X.; Liu, Y.; Chen, C. Ammonium Removal Pathways and Microbial Community in GAC-Sand Dual Media Filter in Drinking Water Treatment. *J. Environ. Sci.* **2012**, *24*, 1587–1593. [[CrossRef](#)]
13. Zhang, J.; Wang, Q. Sustainable Mechanisms of Biochar Derived from Brewers' Spent Grain and Sewage Sludge for Ammonia-Nitrogen Capture. *J. Clean. Prod.* **2016**, *112*, 3927–3934. [[CrossRef](#)]
14. Guieysse, B.; Norvill, Z.N. Sequential Chemical–Biological Processes for the Treatment of Industrial Wastewaters: Review of Recent Progresses and Critical Assessment. *J. Hazard. Mater.* **2014**, *267*, 142–152. [[CrossRef](#)]
15. Rajaniemi, K.; Hu, T.; Nurmesniemi, E.-T.; Tuomikoski, S.; Lassi, U. Phosphate and Ammonium Removal from Water through Electrochemical and Chemical Precipitation of Struvite. *Processes* **2021**, *9*, 150. [[CrossRef](#)]
16. Patel, H. Fixed-Bed Column Adsorption Study: A Comprehensive Review. *Appl. Water Sci.* **2019**, *9*, 45. [[CrossRef](#)]
17. Siyal, A.A.; Shamsuddin, M.R.; Khan, M.I.; Rabat, N.E.; Zulfiqar, M.; Man, Z.; Siame, J.; Azizli, K.A. A Review on Geopolymers as Emerging Materials for the Adsorption of Heavy Metals and Dyes. *J. Environ. Manag.* **2018**, *224*, 327–339. [[CrossRef](#)]

18. Luukkonen, T.; Věžníková, K.; Tolonen, E.T.; Runtti, H.; Yliniemi, J.; Hu, T.; Kemppainen, K.; Lassi, U. Removal of Ammonium from Municipal Wastewater with Powdered and Granulated Metakaolin Geopolymer. *Environ. Technol.* **2018**, *39*, 414–423. [[CrossRef](#)]
19. Gao, Y.; Zhang, J. Chitosan Modified Zeolite Molecular Sieve Particles as a Filter for Ammonium Nitrogen Removal from Water. *Int. J. Mol. Sci.* **2020**, *21*, 2383. [[CrossRef](#)]
20. Sprynskyy, M.; Lebedynets, M.; Terzyk, A.P.; Kowalczyk, P.; Namieśnik, J.; Buszewski, B. Ammonium Sorption from Aqueous Solutions by the Natural Zeolite Transcarpathian Clinoptilolite Studied under Dynamic Conditions. *J. Colloid Interface Sci.* **2005**, *284*, 408–415. [[CrossRef](#)]
21. Lee, W.; Yoon, S.; Choe, J.K.; Lee, M.; Choi, Y. Anionic Surfactant Modification of Activated Carbon for Enhancing Adsorption of Ammonium Ion from Aqueous Solution. *Sci. Total Environ.* **2018**, *639*, 1432–1439. [[CrossRef](#)]
22. Sarkar, C.; Basu, J.K.; Samanta, A.N. Removal of Ni²⁺ Ion from Waste Water by Geopolymeric Adsorbent Derived from LD Slag. *J. Water Process Eng.* **2017**, *17*, 237–244. [[CrossRef](#)]
23. Luhar, I.; Luhar, S.; Mustafa, M.; Abdullah, A.B.; Razak, R.A.; Vizureanu, P.; Sandu, A.V.; Matasaru, P.-D. Materials A State-of-the-Art Review on Innovative Geopolymer Composites Designed for Water and Wastewater Treatment. *Materials* **2021**, *14*, 7456. [[CrossRef](#)] [[PubMed](#)]
24. Ge, Y.; Yuan, Y.; Wang, K.; He, Y.; Cui, X. Preparation of Geopolymer-Based Inorganic Membrane for Removing Ni²⁺ from Wastewater. *J. Hazard. Mater.* **2015**, *299*, 711–718. [[CrossRef](#)] [[PubMed](#)]
25. Al-Harashsheh, M.S.; Al Zboon, K.; Al-Makhadmeh, L.; Hararah, M.; Mahasneh, M. Fly Ash Based Geopolymer for Heavy Metal Removal: A Case Study on Copper Removal. *J. Environ. Chem. Eng.* **2015**, *3*, 1669–1677. [[CrossRef](#)]
26. Ahmaruzzaman, M. A Review on the Utilization of Fly Ash. *Prog. Energy Combust. Sci.* **2010**, *36*, 327–363. [[CrossRef](#)]
27. Provis, J.L.; Van Deventer, J.S.J. *Geopolymers: Structures, Processing, Properties and Industrial Applications*; CRC Press: Boca Raton, FL, USA, 2009; pp. 1–454. [[CrossRef](#)]
28. Sundhararasu, E.; Tuomikoski, S.; Runtti, H.; Hu, T.; Varila, T.; Kangas, T.; Lassi, U. Alkali-Activated Adsorbents from Slags: Column Adsorption and Regeneration Study for Nickel(II) Removal. *ChemEngineering* **2021**, *5*, 13. [[CrossRef](#)]
29. Tunali Akar, S.; Koc, E.; Sayin, F.; Kara, I.; Akar, T. Design and Modeling of the Decolorization Characteristics of a Regenerable and Eco-Friendly Geopolymer: Batch and Dynamic Flow Mode Treatment Aspects. *J. Environ. Manag.* **2021**, *298*, 113548. [[CrossRef](#)]
30. Guo, X.; Zeng, L.; Jin, X. Advanced Regeneration and Fixed-Bed Study of Ammonium and Potassium Removal from Anaerobic Digested Wastewater by Natural Zeolite. *J. Environ. Sci.* **2013**, *25*, 954–961. [[CrossRef](#)]
31. Wang, H.; Gui, H.; Yang, W.; Li, D.; Tan, W.; Yang, M.; Barrow, C.J. Ammonia Nitrogen Removal from Aqueous Solution Using Functionalized Zeolite Columns. *Desalin. Water Treat.* **2014**, *52*, 753–758. [[CrossRef](#)]
32. Irannajad, M.; Kamran Haghghi, H. Removal of Heavy Metals from Polluted Solutions by Zeolitic Adsorbents: A Review. *Environ. Processes* **2021**, *8*, 7–35. [[CrossRef](#)]
33. Chen, Y.; Tian, Q.; Chen, B.; Shi, X.; Liao, T. Preparation of Lithium Carbonate from Spodumene by a Sodium Carbonate Autoclave Process. *Hydrometallurgy* **2011**, *109*, 43–46. [[CrossRef](#)]
34. Kizito, S.; Wu, S.; Wandera, S.M.; Guo, L.; Dong, R. Evaluation of Ammonium Adsorption in Biochar-Fixed Beds for Treatment of Anaerobically Digested Swine Slurry: Experimental Optimization and Modeling. *Sci. Total Environ.* **2016**, *563–564*, 1095–1104. [[CrossRef](#)]
35. de Franco, M.A.E.; de Carvalho, C.B.; Bonetto, M.M.; Soares, R.d.P.; Féris, L.A. Removal of Amoxicillin from Water by Adsorption onto Activated Carbon in Batch Process and Fixed Bed Column: Kinetics, Isotherms, Experimental Design and Breakthrough Curves Modelling. *J. Clean. Prod.* **2017**, *161*, 947–956. [[CrossRef](#)]
36. Fadzail, F.; Hasan, M.; Ibrahim, N.; Mokhtar, Z.; Yekti, A.; Asih, P.; Syafiuddin, A. Adsorption of Diclofenac Sodium Using Low-Cost Activated Carbon in a Fixed-Bed Column. *Biointerface Res. Appl. Chem.* **2022**, *12*, 8042–8056. [[CrossRef](#)]
37. Chu, K.H. Breakthrough Curve Analysis by Simplistic Models of Fixed Bed Adsorption: In Defense of the Century-Old Bohart-Adams Model. *Chem. Eng. J.* **2020**, *380*, 122513. [[CrossRef](#)]
38. Mosanefi, S.; Alavi, N.; Eslami, A.; Saadani, M.; Ghavami, A. Ammonium Removal from Landfill Fresh Leachate Using Zeolite as Adsorbent. *J. Mater. Cycles Waste Manag.* **2021**, *23*, 1383–1393. [[CrossRef](#)]
39. Thomas, H.C. Heterogeneous Ion Exchange in a Flowing System. *J. Am. Chem. Soc.* **1944**, *66*, 1664–1666. [[CrossRef](#)]
40. Vera, M.; Juela, D.M.; Cruzat, C.; Vanegas, E. Modeling and Computational Fluid Dynamic Simulation of Acetaminophen Adsorption Using Sugarcane Bagasse. *J. Environ. Chem. Eng.* **2021**, *9*, 105056. [[CrossRef](#)]
41. Bohart, G.S.; Adams, E.Q. Some Aspects of the Behavior of Charcoal with Respect to Chlorine. *J. Am. Chem. Soc.* **1920**, *42*, 523–544. [[CrossRef](#)]
42. Yoon, Y.H.; Nelson, J.H. Application of Gas Adsorption Kinetics—II. A Theoretical Model for Respirator Cartridge Service Life and Its Practical Applications. *Am. Ind. Hyg. Assoc. J.* **1984**, *45*, 517–524. [[CrossRef](#)]
43. Ali, I.O.; El-Sheikh, S.M.; Salama, T.M.; Bakr, M.F.; Fodial, M.H. Controllable Synthesis of NaP Zeolite and Its Application in Calcium Adsorption. *Sci. China Mater.* **2015**, *58*, 621–633. [[CrossRef](#)]
44. Jin, Y.; Liu, Z.; Han, L.; Zhang, Y.; Li, L.; Zhu, S.; Li, Z.P.; Wang, D. Synthesis of Coal-Analcime Composite from Coal Gangue and Its Adsorption Performance on Heavy Metal Ions. *J. Hazard. Mater.* **2022**, *423*, 127027. [[CrossRef](#)] [[PubMed](#)]
45. Runtti, H.; Tynjälä, P.; Tuomikoski, S.; Kangas, T.; Hu, T.; Rämö, J.; Lassi, U. Utilisation of Barium-Modified Analcime in Sulphate Removal: Isotherms, Kinetics and Thermodynamics Studies. *J. Water Process Eng.* **2017**, *16*, 319–328. [[CrossRef](#)]

46. An, Q.; Li, Z.; Zhou, Y.; Meng, F.; Zhao, B.; Miao, Y.; Deng, S. Ammonium Removal from Groundwater Using Peanut Shell Based Modified Biochar: Mechanism Analysis and Column Experiments. *J. Water Process Eng.* **2021**, *43*, 102219. [[CrossRef](#)]
47. Nguyen, L.H.; Vu, T.M.; Le, T.T.; Trinh, V.T.; Tran, T.P.; Van, H.T. Ammonium Removal from Aqueous Solutions by Fixed-Bed Column Using Corncob-Based Modified Biochar. *Environ. Technol.* **2019**, *40*, 683–692. [[CrossRef](#)]
48. Vu, M.T.; Chao, H.P.; Van Trinh, T.; Le, T.T.; Lin, C.C.; Tran, H.N. Removal of Ammonium from Groundwater Using NaOH-Treated Activated Carbon Derived from Corncob Wastes: Batch and Column Experiments. *J. Clean. Prod.* **2018**, *180*, 560–570. [[CrossRef](#)]
49. Franchin, G.; Pesonen, J.; Luukkonen, T.; Bai, C.; Scanferla, P.; Botti, R.; Carturan, S.; Innocentini, M.; Colombo, P. Removal of Ammonium from Wastewater with Geopolymer Sorbents Fabricated via Additive Manufacturing. *Mater. Des.* **2020**, *195*, 109006. [[CrossRef](#)]
50. Xiong, S.; Ma, L.; Jiang, L.; Hu, X.; Fu, G.; Hao, J.; Gao, H.; Liu, P.; Tan, L.; Liu, X.; et al. Low-grade sepiolite with low loading of Na/La salts for simultaneous removal of ammonia and phosphate from wastewater. *J. Sci. Environ.* **2023**, *858*, 160127. [[CrossRef](#)]
51. Samarina, T.; Guagneli, L.; Takaluoma, E.; Tuomikoski, S.; Pesonen, J.; Laatikainen, O. Ammonium recovery by combined adsorption and air-stripping approach from wastewaters. *Front. Environ. Sci.* **2022**, *10*, 1033677. [[CrossRef](#)]
52. Karadag, D.; Akkaya, E.; Demir, A.; Saral, A.; Turan, M.; Ozturk, M. Ammonium removal from municipal landfill leachate by clinoptilolite bed columns: Breakthrough modeling and error analysis. *Ind. Eng. Chem. Res.* **2008**, *47*, 9552–9557. [[CrossRef](#)]
53. Mashal, A.; Abu-Dahrieh, J.; Ahmed, A.A.; Oyedele, L.; Haimour, N.; Al-Haj-Ali, A.; Rooney, D. Fixed-Bed Study of Ammonia Removal from Aqueous Solutions Using Natural Zeolite. *World J. Sci. Technol. Sustain. Dev.* **2014**, *11*, 144–158. [[CrossRef](#)]
54. Halim, A.A.; Hanafiah, M.M.; Khairi, A. Ammonia Removal from Sewage Wastewater Using Chemically Modified Sand. *Appl. Ecol. Environ. Res.* **2017**, *15*, 521–528. [[CrossRef](#)]